Materials Letters 209 (2017) 547–550

Contents lists available at ScienceDirect

Materials Letters

journal homepage: www.elsevier.com/locate/mlblue

Binder-free TiO_2 nanowires-C/Si/C 3D network composite as high performance anode for lithium ion battery

Wenjuan Liao, Dingqiong Chen, Yiyong Zhang, Jinbao Zhao *

College of Chemistry and Chemical Engineering, State Key Laboratory of Physical Chemistry of Solid Surfaces, Collaborative Innovative Center of Chemistry for Energy Materials, State-Province Joint Engineering Laboratory of Power Source Technology for New Energy Vehicle, Xiamen University, Xiamen 361005, China

ARTICLE INFO

Article history:
Received 9 June 2017
Received in revised form 12 August 2017
Accepted 21 August 2017
Available online 31 August 2017

Keywords:
Lithium-ion battery
Silicon
Binder-free anode
Chemical vapor deposition
Nanocomposite

ABSTRACT

Silicon has been considered as the most promising anode candidate of new generation high-performance LIBs, but the huge volume strain during cycling processes limited its practical applications. Herein, the binder free TiO_2-nanowires (NWs)-C/Si/C 3D network composite has been prepared by chemical vapor deposition (CVD) and facile carbonization process as a great solution to the problem. In this composite, the intertwined TiO_2-NWs serves as a buffer matrix to alleviate the volume strain of silicon during cycling processes, while the dual protective carbon layers enhance the conductivity of TiO_2-NWs and prevent Si from peeling off the substrate. The as-prepared TiO_2-NWs-C/Si/C anode shows great cycling performance with a reversible capacity of 1570 mAh g^{-1} at 2 A g^{-1} and excellent capacity retention of 85.7% up to 100 cycles.

1. Introduction

Lithium ion batteries (LIBs) as environmentally friendly energy conversion and storage systems become the focus of researches in recently years [1,2]. In response to the growing energy requirement, research efforts are mainly focused on searching for materials with higher energy density and prolonged cycle life. Silicon owns appreciable capacity up to 3572 mAh g^{-1} [3], low work potential and natural abundance, which makes it becomes the most promising and commercially viable anode candidate of new generation high-performance LIBs. However, there are still crushing problems to address before practical applications. Huge volume expansion (~300%) of silicon causes electrode structure pulverization and eventually leads to quick capacity fading [4].

The two solutions mainly reported are fabricating nanostructure and Si-base composites. On the one hand, the complicated nanostructures could alleviate the huge expansion impacts. On the other hand, the introduction of the conductive and chemically stable materials efficiently improves the conductivity of the composites and withstands the volumetric strain during cycling. In addition to the materials, current collector also has the important effect on the electrochemical performance of LIBs [5]. The current collector with roughness surface especially three-dimensional (3D) structure has stronger adhesion and much enhanced electrical contact with silicon than smooth foil [6], which avoids active materials falling off the collector and hence brings about effectively improvement in electrochemical performance [7].

In this paper, we take both the material and the current collector into consideration and design a binder-free TiO_2-NWs-C/Si/C 3D network composite. The intertwined TiO_2-NWs grown on Ti foil is selected as roughness current collector and buffer matrix due to its robust structural stability and easy preparation. The dual carbon layers are introduced to improve the electronic conductivity and structural stability of the electrode. We confine silicon nanoparticles into this continuous conductive matrix via chemical vapor deposition (CVD) process, to fabricate a binder free electrode which could alleviate the electron conductivity loss owing to the low conductivity of traditional binder. Therefore, the finally obtained TiO_2-NWs-C/Si/C composite is expected to present excellent electrochemical performance.

2. Experimental

The TiO_2-NWs on Ti foil was synthesized according to the previously reported work [8] and then punched into 12 mm diameter electrodes. 0.1 g glucose powder was dispersed in 10 ml water, the mixture was put into a Teflon-lined autoclave with several pieces of TiO_2-NWs electrodes then heated to 200 °C for 12 h. The obtained TiO_2-NWs-glucose electrode was washed with water and dried, followed by a CVD process accompanied with glucose carbonization. The deposition parameters were 10% SiH_4 (diluted

---

* Corresponding author.
E-mail address: jbzhao@xmu.edu.cn (J. Zhao).

http://dx.doi.org/10.1016/j.matlet.2017.08.084
0167-577X/© 2017 Elsevier B.V. All rights reserved.

by Ar), flow rate 10/30 sccm of H_2/SiH_4, temperature 650 °C. Subsequently, 0.5 g/ml PEG in ethanol was dropped on the as-prepared TiO_2-NWs-C/Si electrode and heated to 450 °C under the argon atmosphere to attain TiO_2-NWs-C/Si/C 3D network electrode. We also prepared TiO_2-NWs/Si (Si was in-situ directly grown on TiO_2-NWs) for comparison.

X-ray diffraction (XRD) spectrums were used to characterize the crystal structure on Rigaku UiniFlex 600 with Cu Kα radiation, in the rage of 10°–90°. Morphologies characterization were carried out on scanning electron microscopy (HITACHI S-4800). Raman spectrums were obtained using a JOBIN Yvon Horiba HR800.

The materials we prepared can directly use as a working electrode without binder and making slurry. The coin type half cells were assembled in an argon-filled glove box with metallic lithium foil as the counter electrode and Celgard 2400 as the separator. 1 M $LiPF_6$ in EC/DEC/DMC 1:1:1 v/v/v mixture with 5 wt% fluorinated ethylene carbonate additive was used as the electrolyte. The charge/discharge test was performed between 0.02 and 1.5 V (vs Li^+/Li) by using the LAND-CT2001A battery test system. Cyclic voltammetry (CV) was carried out at the scan rate of 0.01 mV^{-1} with the CHI660D electrochemical workstation.

3. Results and discussion

The XRD analysis of TiO_2-NWs/Si and TiO_2-NWs-C/Si/C recorded in Fig. 1a. The sharp diffraction peaks appear at 28.5°, 47.3°, 56.1°, 69.1°, 76.4° and 88.0° of both two samples, these peaks can be indexed to crystalline Si (JCPDS No. 00-0260-1481). The other diffraction peaks are all originated from anatase-phase TiO_2 (JCPDS No. 01-089-4921) and metallic Ti (JCPDS No. 01-089-2762), implying that silicon is deposited on TiO_2-NWs without producing alloys or other impurities. There are no detected peaks assignable to crystalline carbon in all patterns, indicating the amorphous structure of carbon, which agrees well with previous work [9]. The existence of amorphous carbon was further confirmed through Raman spectroscopy (Fig. 1b). For both two samples, strong peaks at 520 cm^{-1} and 960 cm^{-1} were detected, indicating the vibration of crystalline Si. Two weak broad peaks at 1350 and 1605 cm^{-1} in TiO_2-NWs-C/Si/C are attributed to the D band (disorder amorphous carbon) and G band (ordered graphite), respectively [10]. The I_D/I_G ratio of TiO_2-NWs-C/Si/C is 0.91, indicating that the carbon in the composite is mainly composed of amorphous carbon, which is consistent with XRD result.

Fig. 2 displays morphology images of as-prepared samples. As illustrated in Fig. 2a, the diameters of TiO_2-NWs are mainly 50–70 nm, and lots of intertwined non-oriented nanowires form a three-dimensional network. From Fig. 2b, we can find that the TiO_2-NWs/Si composite still maintains the network structure and the silicon nanoparticles are evenly and loosely dispersed on the surface of TiO_2-NWs. Fig. 2c shows the structure of TiO_2-NWs-C/Si/C composite. The carbon layer makes part of the TiO_2-NWs clustered together and then obtains a terrace like construct. We can see more clearly from the amplifying figure, the silicon particles tightly compact with each other with a diameter of approximately 150 nm, and form a silicon film coating onto TiO_2-NWs-C substrate, indicating an obviously reinforce of adhesion and electrical contact between the substrate and silicon. The TEM image of TiO_2-NWs-C/Si/C reveals that TiO_2-NWs are mutually interlaced and the silicon particles are uniformly dispersed into the network (Fig. 2d). This kind of network structure could provide a continuous electron conductive network, and buffer space for accommodating volume expansion of silicon. The morphology of a single nanowire coated with silicon and carbon is presented in Fig. 2e. The HRTEM image shows in Fig. 2f, the interlayer spacing of 0.31 nm is consistent with the (1 1 1) planes of silicon and the outer space without lattice fringes is attributed to amorphous carbon.

The first three CV curves of the TiO_2-NWs-C/Si/C electrode is shown in Fig. 3a. The cathodic peak at 0.1 V is attributed to the formation of amorphous Li-Si phase and/or crystallization of $Li_{15}Si_4$ phase, and gradually shift to 0.2 V implying the transformation of crystalline Si to amorphous Si. The anodic peaks at 0.36 and 0.51 V are associated with the de-alloying of amorphous Li-Si phase [11]. The redox peaks at 1.65 and 2.15 V corresponding to the lithium insertion and extraction of TiO_2. It is further confirmed that TiO_2 is inactive component below 1.5 V and only serves as a conductor and buffer matrix. The advantage of the unique structure is evident from the great electrochemical behavior. If not mentioned, all the capacities reported are calculated on the total weight of silicon and carbon, in which the mass of silicon is controlled between 0.6 and 0.8 mg. The initial charge-discharge voltage curves of the composites at the current density of 0.5 A g^{-1} (0.2 C) are shown in Fig. 3b. The initial discharge capacities of TiO_2-NWs/Si and TiO_2-NWs-C/Si/C anodes are 2486 and 2200 mAh g^{-1}, corresponding to the first cycle coulombic efficiency of 82% and 87%, respectively. Fig. 3c shows the cycle performance of the electrodes at the high current density of 2 A g^{-1} (in initial 3 cycles at 0.2 A g^{-1}). The TiO_2-NWs/Si shows a rapid decline during the beginning cycles and only 58% capacity retention up to 100 cycles. While the TiO_2-NWs-C/Si/C maintains the capacity of 1570 mAh g^{-1} after 100 cycles with the great capacity retention

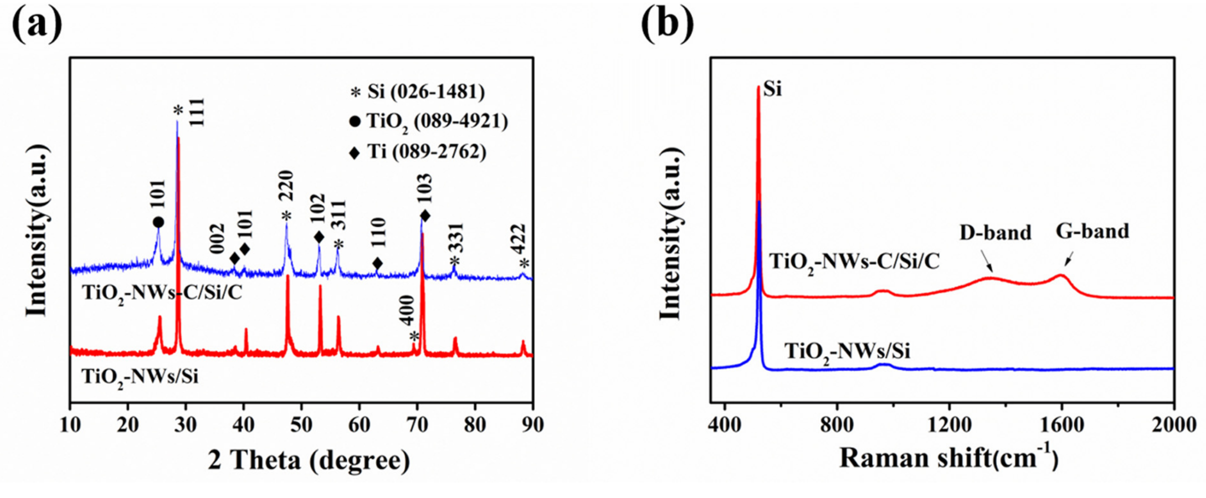

Fig. 1. (a) XRD patterns and (b) Raman spectra of TiO_2-NWs/Si and TiO_2-NWs-C/Si/C composites.

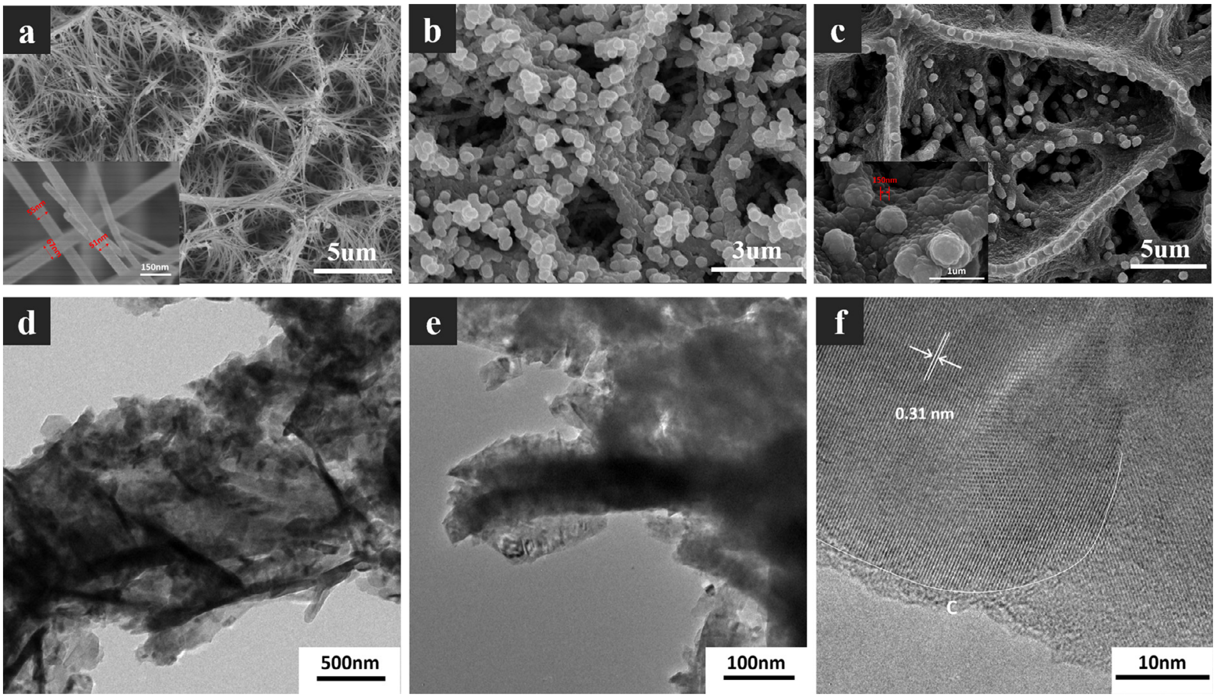

Fig. 2. SEM images of the as-prepared (a) TiO_2-NWs, (b) TiO_2-NWs/Si, (c) TiO_2-NWs-C/Si/C; (d, e) TEM images of TiO_2-NWs-C/Si/C; (f) HRTEM images of Si in TiO_2-NWs-C/Si/C.

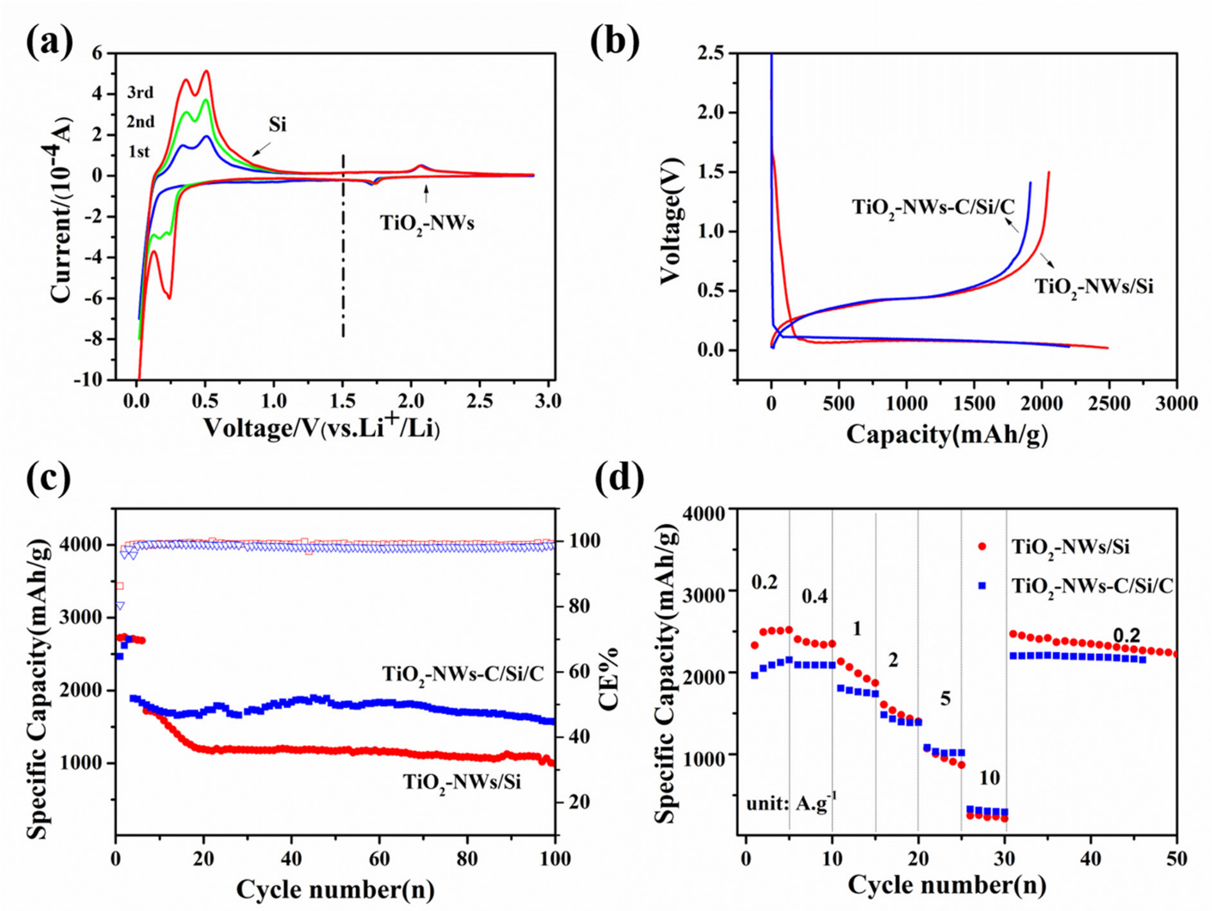

Fig. 3. (a) CV curves of the TiO_2-NWs-C/Si/C electrode; (b) Initial discharge-charge voltage profiles, (c) Cycling performance at a 2 A g^{-1}, (d) Rate performance of both TiO_2-NWs/Si and TiO_2-NWs-C/Si/C composites.

of 85.6% compared to its first charge capacity at 2 A g^{-1} (the 4th cycle). This demonstrates that the introduction of dual carbon layer can improve the cycle stability of the composites. Fig. 3d illustrates the rate performance of materials from 0.2 to 10 A g^{-1}. For both electrodes, the capacity quickly recovers to the initial value when the current density decreases back to 0.2 A g^{-1}. The TiO_2-NWs-C/Si/C shows greater capacity retention than TiO_2-NWs/Si since 1 A g^{-1} and higher capacity since 5 A g^{-1}, implying a better rate performance at high current densities.

4. Conclusion

The binder-free TiO_2-NWs-C/Si/C 3D network composite has been successfully fabricated via chemical vapor deposition and facile carbonization process. In this unique structure, TiO_2-NWs plays an important role in stabilizing the structure of the material since its intertwined network structure provides enough buffer space to accommodate the volume change of silicon during cycling processes. The introduction of the dual carbon coating layers has significantly improved the conductivity of TiO_2-NWs and enhanced the adhesion between the silicon and the matrix. Therefore, as the anode material, the TiO_2-NWs-C/Si/C electrode shows a great electrochemical performance.

Acknowledgements

This work was supported by the National Natural Science Foundation of China (grant numbers: 21273185, 21321062) and Key Project of Science and Technology of Xiamen (grant number: 3502Z20141008).

References

[1] A.S. Arico, P. Bruce, B. Scrosati, J.M. Tarascon, Nat. Mater. 4 (2005) 366–377.
[2] G. Zhu, K. Wen, W. Lv, J. Power Sources 300 (2015) 29–40.
[3] C.K. Chan, H. Peng, G. Liu, et al., Nat. Nanotechnol. 3 (2008) 31–35.
[4] Z. Li, Q. He, L. He, et al., J. Mater. Chem. A 5 (2017) 4183–4189.
[5] B. Wang, X. Li, B. Luo, Y. Jia, Nanoscale 5 (2013) 1470–1474.
[6] J. He, P. Li, W. Lv, Electrochim. Acta 215 (2016) 12–18.
[7] Y.L. Kim, Y.K. Sun, S.M. Lee, Electrochim. Acta 53 (2008) 4500–4504.
[8] H. Lin, X. Li, X. He, J. Zhao, Electrochim. Acta 173 (2015) 242–251.
[9] Y.S. Hu, R. Demir-Cakan, M.M. Titirici, et al., Angew. Chem. Int. Ed. Engl. 47 (2008) 1645–1649.
[10] M. Zhou, T. Cai, F. Pu, H. Chen, et al., ACS Appl. Mater. Interfaces 5 (2013) 3449–3455.
[11] D. Chen, W. Liao, Y. Yang, J. Zhao, J. Power Sources 315 (2016) 236–241.